SAND20XX-XXXXR SAND2016-9915R

LDRD PROJECT NUMBER: 192869

LDRD PROJECT TITLE: Modeling Electric Double Layer Effects on Charge Transfer at Flow Battery Electrode/Electrolyte Interfaces

PROJECT TEAM MEMBERS: Kevin Leung (1131, PI), Ray Shan (1814); Amy C. Sun (1814, PM)

ABSTRACT

The proposal aims to model interfacial processes associated with redox flow batteries (RFB) for grid/stationary storage, with the ultimate goal of helping design new electrolytes, electrodes, redox species, and interfaces. It addresses the linked problems of electric double layer (EDL) structure and electron transfer at model electrode/electrolyte interfaces. Fast electron transfer partly determines which redox species are viable for flow batteries (along with solubility, viscosity, etc.). Commercial systems apply aqueous, vanadium-based complexes, but other choices and organic electrolytes with larger voltage windows are the subject of active research at Sandia and elsewhere. The high salt concentration present in flow battery electrolytes yields non-trivial EDL consisting of solvents, counter-ions, co-ions, and redox species (at different charge states at the charging voltage threshold). EDL strongly influences electron transfer, especially when redox "mediators" are used. Modeling this key missing information is the main challenge. Our proposal seeks to apply Sandia's LAMMPS molecular dynamics code. As a proof of principle, we study minimal model systems (graphite electrode, with ferrocene and fluornone as redox-active species). These model "catholyte" and "anolyte" molecules exhibit low reorganization energies (in the sense of Marcus theory) and are most amenable to EDL simulations which involve switching of redox states to mimic electron transfer. This study will enable future modeling and design of redox species relevant to flow batteries and redox mediators used at Sandia for other purposes.

1. INTRODUCTION

(a) Redox Flow Batteries

The use of rechargeable batteries for stationary electrical energy storage will facilitate

the incorporation of solar and wind generation of electricity into the electrical grid. The intermittent renewable energy generated during sunlit and/or windy hours can be temperorily stored and then released to stabilize the the power supplied to the grid; it can also be released during evening peak hours. For this purpose, it is important to develop inexpensive, scalable, and reliable electrical energy storage technology.

Redox Flow batteries (henceforth referred to as RFB or "flow batteries") constitute a technology designed for large scale storage.[1] Flow batteries involve liquid "catholytes" and "anolytes" that can be charged and then pumped into vats for storage. When the need arises, they are pumped back to the electrode for discharge and to release energy. Hence capacity and kinetics are decoupled. Some requirements of flow battery redox-active species are high solubility, high charge transfer rate, low viscosity, and reliability. Currently vanadium-based aqueous flow batteries are the most commercially ready.[2] The cutting edge basic research is on flow batteries based on non-aqueous electrolytes, which can support a larger voltage window than water ($\sim$ 1.2 V), and can potentially enable the use of catholyte and anolyte molecules that support multi-electron transfer. Critical issues associated with such organic electrolyte systems include rapid capacity loss (degradation), high viscosity, separator membrane performance, and cost.[3] The charge transfer rate at electrode/electrolyte interfaces should be high to compensate for the typically one order of magnitude higher viscosity of organic liquids compared to water used in vanadium flow batteries.[3,4] The charge transfer rate used in different economics analysis of flow battery viability can differ by as much as a factor of 30.[3] The ability to model such rates accurately, or at least to compare the rate between different redox species, would be beneficial for many aspects of flow battery design and development.

(b) Modeling Electrochemistry without electronic structure

Atomic lengthscale modeling of flow battery components is in its infancy. Modeling of the separator membrane and the redox potentials of catholytes/anolytes have generally applied electronic structure ("quantum mechanics" or Density Functional Theory/"DFT") calculations.[5] However, studies that involve the multicomponent liquid electrolyte require thousands of atoms, nanometer lengthscales, and nanosecond timescales. These are too costly for electronic structure calulations. This is particularly true when modeling electrode/electrolyte interfaces which control charge transfer events. The interfacial region is also likely to play key role to organic electrolyte degradation events during charge/discharge

processes. To our knowledge, while the transport propertiess of flow battery electrolytes have been simulated in the bulk liquid phase,[6] electode/electrolyte interfaces have not been the subject of atomic lengthscale modeling. Even the conceptual framework of such modeling effort has arguably not been established.

Our goals are to model flow battery electrode/electrolyte interfaces to gain insights and elucidate design principles. Since the separator is supposed to block cross-talk between anolytes and catholyes, our simulations focus on one electrode at a time, with the two electrodes dealt with in separate simulation cells.

A second theme of this project is to enable simulations of electrochemical interfaces without costly all-atom electronic structure calculations. The ability to perform such simulations will benefit not just flow batteries, but also other energy storage and related devices relevant to the Department of Energy and Sandia National Laboratories. For the purpose of modeling flow batteries, we seek to establish and apply a simulation protocol dealing with the two following processes. (1) Lower the voltage of the anode in contact with discharged anolyte, until the reduction potential is reached. (2) Model the sequential charge transfer to anolyte until it is 100% reduced. (3) Modeling of the cathode/catholyte interface is analogous.

Following Ref. 7, we consider modified Fc with one $N(CH_3)_3^+$ group replacing a hydrogen. This modified Fc is called Fc' henceforth. A similar modification has been shown to have a $2-4$ molar solubility in organic solvents.[7] High redox species concentrations are critical to designing flow batteries with reasonable capacity. Fluornone (Fl), which has been examined as redox-active anolyte,[8] is adopted as the model anolyte.

2. METHOD

This work apply mostly classical forcefield (non-electronic) molecular dynamics ("CFMD" or just "MD"), augmented by some electronic DFT calculations, to study interfaces relevant to flow batteries. In order to capture electrochemical conditions and electron transfer events with very little electronic structure input, the following are needed (Fig. 1):

(a) DFT calculations of electrode (graphite basal plane) work function in vacuum, plus the electron affinity of the anolyte or the ionization potential of the catholyte;

(b) CFMD calculation of voltage at charge-neutral electrode/electrolyte interfaces (i.e., at potential-of-zero-charge or PZC), to add solvent effects to the DFT work function;

(c) CFMD simulations of electric double layer with net charges on electrode surfaces to control the voltage;

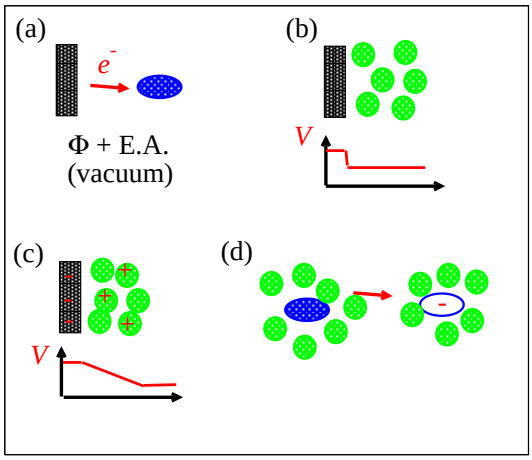

FIG. 1: The four steps used to model interfacial charge transfer without performing all-atom electronic structure calculations (see text).

(d) CFMD "vertical gap" calculations along the MD trajectory for Marcus theory-type electron transfer rate estimates. As a by-product, solvation free energies needed for computing absolute voltages are obtained. These are conducted both at interfaces and in bulk liquid environments.

Gas phases electronic calculations are conducted using the g09 suite of programs.[9] Their main purpose are to provide optimized structures and partial atomic charges for MD simulations. Solution phase *ab initio* molecular dynamics (AIMD) simulations, based on DFT-generated forces, are applied to explore modified Fc', Fc'^{+}, Fl, Fl^{-}, and Fl^{2-} solvation structures and possible reaction with acetonitrile (CH_3CN) solvent molecules. The VASP code and the PBE functional are applied.[10–12]

The Sandia LAMMPS code is used to conduct CFMD simulations. Special code modifications are applied when CFMD is conducted in solid-liquid interface environments (Fig. 2). Here the simulation cell has one real electrode (the leftmost, 4-layer graphite slab) and one fictitious electrode (rightmost, one-layer graphite). The right-side electrode is charge neutral and exists only to prevent the liquid electrolyte from evaporating. A constant potential

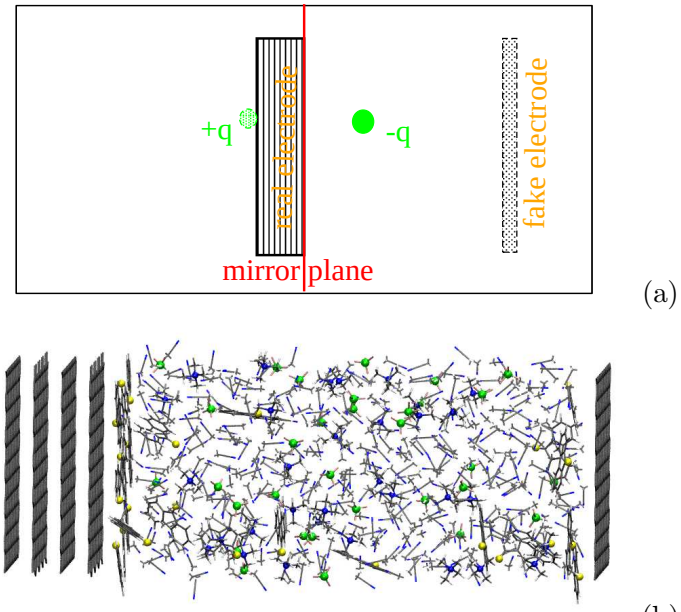

FIG. 2: (a) Illustration of electrode/electrolyte interface simulation cell. The dividing surface for image charges is always at the center of the cell. (b) Actual snapshot of simulation. Only the left-side electrode (4 layers of graphite) is a real electrode; the right side single carbon sheet only serves to prevent liquid evaporation. The electrolyte is a mix of BF_4^-, $N(CH_3)_4^+$, Fl, and Fl^- in CH_3CN solvent.

condition – keeping the electrode surface at the same potential – is more appropriate than the commonly used constant charge simulation condition. The "image-charge" approach is used for this purpose.[13]

This approach is implemented as follows. A dividing surface is placed on the left-side innermost graphite sheet. Each atomic charge q_i on atom i of either solvent or ionic molecules at a distance z_i in front of the dividing plae is given a reflected charge of magnitude $-q_i$ at a distance $-z_i$ behind that surface (Fig. 2a). The image charges represent the excess electron/hole surface density on the metallic electrode. By construction, the entire dividing surface is at the same electrostatic (and hence electrochemical) potential. Image charges also ensure that the system is overall charge neutral.

Ewald sum is used to handle long-range electrostatics. Algorithms that combine Ewald and image charges have not been extensively documented in the literature. Here we define the total electrostatic energy to be exactly half of a fictitious system which treat our behind-

the-electrode the image charges as real charges. The forces on real atoms are halved and then doubled, because they and their images are constrained to move in unison. The image-charge voltage V is δV added to the potential-of-zero-charge $V_{\rm pzc}$, where δV is the electric double layer term which depends on the molecule charges:

$$\delta V = 4\pi|e| \sum_i [q_i z_i - q_i(z_p - 2_i)]/2A. \quad (1)$$

Here i sums over both real and image charges, z_p is the z-coordinate of the dividing surface, A is the lateral surface area of the simulation cell, $|e|$ is the electron charge, and the expression is in atomic unit. The factor of one-half exists to reconcile the energy change when an infinitesimal test charge, and its image, are inserted into the system to compute the potential.

While the potential V is constant on the leftmost electrode surface, it fluctuates from CFMD timestep to timestep. In the future, one way to impose a time-independent voltage is to adjust a uniform surface charge on the rightmost fictitious electrode. This can be analytically done at every time step. Recall that only the interface on the left side is used for electric double layer analysis; what happens on the right side is immaterial. However, extensive testing needs to be conducted for this proposed modification before it can be used for production runs.

Note that Voth *et al.* have also implemented image charges into the LAMMPS code. Their modification has not been shared with Sandia. However, in addition to the image charges, they also include a net charge on each electrode. Therefore local charge neutrality – a main consequence of the electric double layer, allowing the electrolyte to neutralize the electrode surface charge – is violated. In the limit that the system size goes to infinity, the net energy of the system would diverge without local charge neutrality. Voth *et al.* manage to avoid this divergence because they only consider a nanoscale, not infinite, system. Our formulation avoids this problem.

The force field used are adapted from Refs. 6 and 14 All molecules are held rigid. Omitting intramoleclar motion greatly simplifies charge transfer simulations.

3. RESULTS

3.1 AIMD simulations of Fc' and Fl in CH_3C

First we apply AIMD simulations on a single redox-active species (Fc' or Fl) in liquid CH_3CN to make sure that the solute can be adequately modelled as a rigid body. AIMD is based on DFT forces and does not freeze internal degrees of freedom, unlike our CFMD

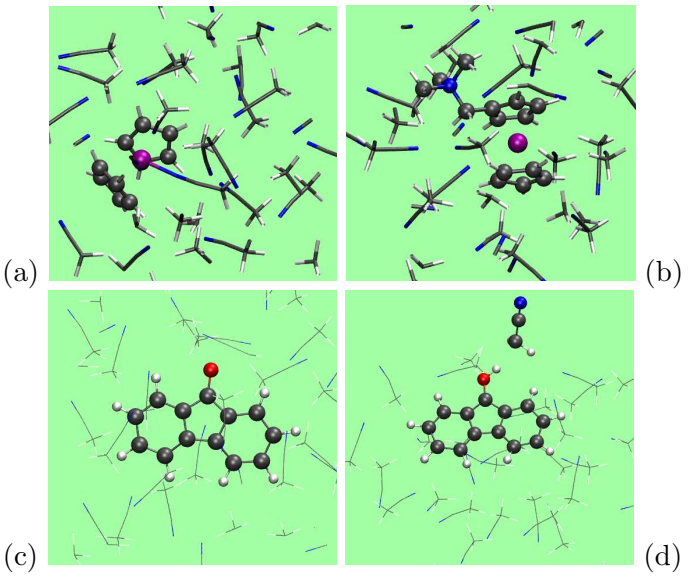

FIG. 3: AIMD simulations of bulk CH_3CN liquid with one solute molecule. (a) Fc'^+ with high-spin Fe(III); (b) Fc'^+ with low-spin Fe(III); (c) Fl^-; (d) Fl^{2-} after abstracting a proton from a CH_3CN.

simulation. Fig. 3a depicts a Fc'^+ in a high spin Fe(III) configuration in solution. High spin was used because this electronic structure configuration minimizes the gas phase energy. Within 4 picosecond (ps), a CH_3CN molecule has "reacted" with Fc'^+. This is contrary to experimental evidence, which states that Fc and its derivatives are stable in solutions. Fig. 3b shows that low-spin Fc'^+ is in contrast very stable against CH_3CN. By imposing this experimental Fe(III) spin state, we determine that it is legitimate to model Fc'^+ as a rigid body.

Fl and Fl^- both exhibit minimal deformation in AIMD simulations in the liquid state (Fig. 3c), and can therefore be approximated as rigid bodies. These simulations also let us examine Fl degradation during battery charging.[8] Neither Fl or Fl^- reacts with CH_3CN, contrary to a conjecture in the literature.[8] However, Fl^{2-} reacts readily and reversibly, abstracting a proton from CH_3CN in picosecond timescale (Fig. 3d). We tentatively conclude that two electron reduction is needed for Fl degradation. An alternate hypothesis is that Fl^- may directly react with the electrode. This will be discussed in later sections.

3.2 CFMD simulations: Fl and Fl^- solvation

The Fl $\rightarrow$ Fl^- change-of-solvation free energy is pertinent to calibrating the electrode surface charge/voltage needed to induce Fl electrochemical reduction. We apply the ther-

modynamic integration (TI) technique to calculate this change:

$$\Delta\Delta G_{\rm solv} = \Delta G_{\rm Fl-solv} - \Delta G_{\rm Flsolv} \quad (2)$$

$$= -\int_0^{-1} dq \langle E(q=-1) - E(q=0)\rangle_q. \quad (3)$$

The subscript on the brackets denote performing a different CFMD trajectory at each partial charge $-q$ on Fl. Using a 6-point integration rule, we find that $\Delta\Delta G_{\rm solv}$=-2.39 eV. Added to the negative of the gas phase Fl electron affinity, calculated to be -1.165 eV, we obtain -3.53 eV. Converted to the Standard Hydrogen Electrode ("SHE") scale, the Fl reduction potential in CH_3CN is predicted to be -0.91 V, close to the -0.97 V vs. SHE reported in measurements. This shows that the CFMD simulations, augmented by DFT gas phase predictions, are capable of yielding the correct solvation effect. We will use the computed -0.91 V value as the Fl reduction potential inn this work.

Also relevant is the distribution of the "energy gap" $\langle E(q=-1) - E(q=0)\rangle_q$ along the end point trajectories, at $q=-1$ and $q=0$. By calculating the curvatures of the logarithms of the distributions, fitting to Marcus theory parabolas, and locating the intersection, the electron transfer barrier due to solvation is determined to be 0.44 eV barrier. No experimental data exists for comparison, but this barrier is likely overestimated because of our neglect of electronic polarizability.

We stress that all these are computed in the absence of the electrode.

3.3 CFMD simulations: electrode-anolyte interface

Next we consider Fl and Fl^- at electrode interfaces, and ask the question: what is the electric double layer structure needed for simulations of battery charging conditions?

Using DFT calculations, the charge-neutral graphite basal plane exhibits a work function of 4.40 eV. Applying CFMD simulations and adding a pure CH_3CN solvent on the charge-neutral graphite basal plane, we find negligable change in the work function (i.e., there is almost no electric double layer). Therefore the voltage of the charge neutral graphite plane in contact with CH_3CN-based electrolyte is assigned to be -0.04 V vs. SHE.

Fig. 4a depicts a snapshot of the CFMD simulation at pzc when redox-active species and co-ions are also present. Fl molecules, which are charge-neutral, lie flat on the charge-neutral graphite basal plane. In this way, van der Waals contact is maximized. δV is -0.05 V from averaging the molecular configurations and applying Eq. 1. In other words, adding Fl and the co-ions hardly changes the pzc=-0.04 V previously computed using the pure CH_3CN

solvent. Adding the work function contribution, the pzc anode potential is -0.09 V. From the discussions in the previous subsection, this potential-of-zero-charge (pzc) on the electrode needs to be lowered to -0.91 V or below to enable Fl reduction to Fl^- by adding negative surface charges.

Therefore we next remove two and then one more BF_4^-, respectively. Because of the image charges induced on the left-side electrode, the latter becomes charge-negative. By averaging Eq. 1, we obtain V= -0.73±0.02 nd -0.88±0.2 V for these anode interfaces with lowered BF^- content. Due the negative image charge on the graphite at these voltages, some Fl molecules become tilted out of the plane to permit close proximity and favorable electrostatic interactions between the graphite and the CH_3CN solvent and $N(CH_3)_4^+$ co-ions (Fig. 4b).

−0.88 V vs. SHE is close to the voltage (-0.91 V) when Fl starts to be reduced to Fl^-. Note that our voltage increments are functions of the discrete number of cations deleted. Smaller voltage increments require simulation cells with larger lateral surface areas, according to Eq. 1. Therefore we assume that we have reached the battery charging threshold at -0.91 V, and that Fl molecules start to transform into Fl^-. In Fig. 4c, one Fl^- lying flat on the electrode surface is replaced with a Fl^-. Within 10 ps, the $O^{\delta-}$ in Fl^- has tilted away from the surface and coordinated to solvent molecules. This underscores the dramatic changes in adsorption gemetry as a function of Fl charge state (not just graphite charge state), arising from the highly asymetric shape of Fl.

Under quasi-equilibrium or slow-charging conditions, the voltage should be pinned at the onset of Fl reduction until the transformation of Fl to Fl^- is completed and all anolyte molecules have accepted a electron. Fig. 4e represents partial reduction of the available Fl. One unreduced Fl molecule remains adsorbed in a flat geometry on the left electrode. Fig. 4d depicts the fully reduced state. All Fl have been reduced to Fl^-. All of them are tilted away from the surface.

The average voltages associated with the Fig. 4d and Fig. 4e trajectories are -0.91±0.01 and -0.88±0.02 V, respectively. In each case, a net $-3|e|$ charge exists on the left electrode as image charge. The voltage is therefore only sensitive to the net charge on the electrode, not the precise composition of the electrolyte. Note that this implies EDL structure will be *very* sensitive to voltage changes, as we have obeserved in Fig. 4.

Finally, Fig. 5 depicts the interfacial structures of a graphite cathode in contact with Fc'

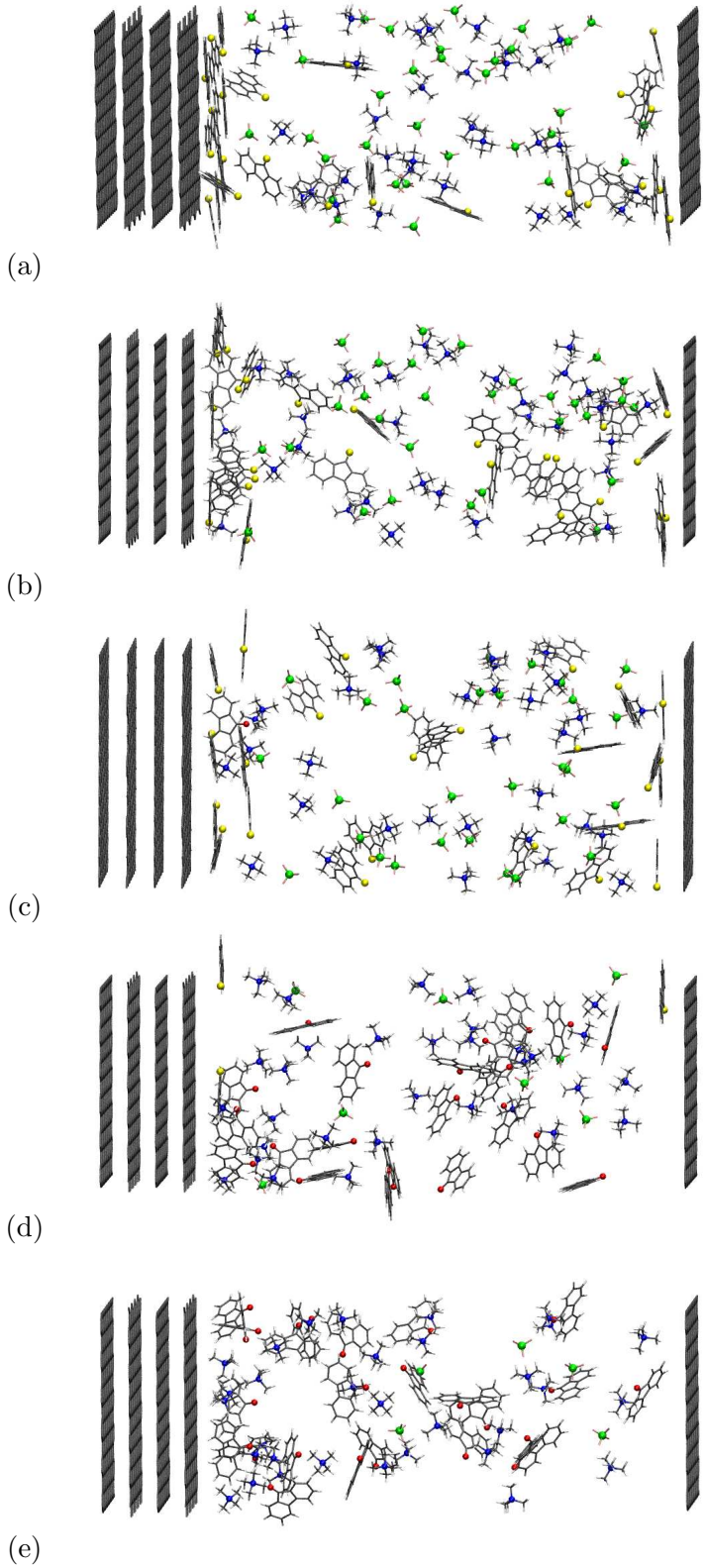

FIG. 4: Snapshots of CFMD simulations of (a) -0.05 V, all Fl; (b) -0.88 V, all Fl; (c) -0.73 V, one adsorbed Fl^-; (d) -0.91 V, two Fl not yet reduced; (e) -0.88 V, all Fl reduced to Fl^-.

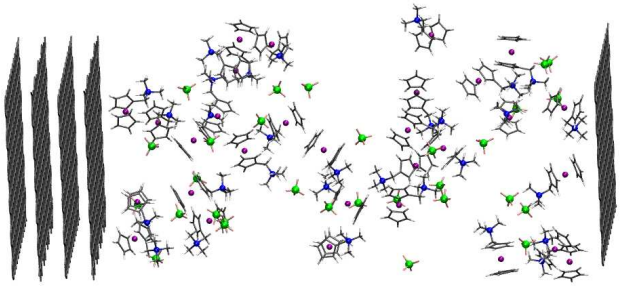

FIG. 5: Snapshot of CFMD simulations of Fc' at graphite electrode interface.

catholyte. The voltage is the pzc (-0.04 V vs. SHE). This is not high enough to oxidize Fc', all of which therefore is constrained to remain in Fe(II) states. The $N(CH_3)_3^+$ pendant is orientated away from the charge-neutral electrode. This is reasonable because this positively charged fragment is expected to be strongly solvated by solvent molecules.

To our knowledge, these electric double layer structures of flow-battery-relevant electrolytes at different voltages are novel, never been discussed in the literature. They will be the basis of a future publication.

3.4 Electron Transfer and Reorganization Energies

The non-adiabatic electron transfer rate associated with a molecule is

$$k_{\rm et} = \frac{\sqrt{\pi}|V_o|^2}{\hbar\sqrt{\lambda k_{\rm B}T}} \exp\left[-\frac{(\eta+\lambda)^2}{4\lambda k_{\rm B}T}\right]. \tag{4}$$

Here η is the overpotential, set to zero under the quasi-equilibrium considered under our simulation conditions. The most important quantities are the coupling matrix element V_o between the donar/acceptor orbitals, and the reorganization (free) energy λ. V_o couples the donor and acceptor orbitals, and is a function of the e^- tunneling distance and molecular orientation. λ represents the change in intramolecular and intermolecular deformation cost for the molecule to absorb or release an electron. For rigid molecules like Fl and Fc', intramolecular components are small ($\sim$0.1 eV) and are neglected in this work. Small λ facilitates electron transfer and is one of the reasons rigid organic or organometallic molecules have been used in laboratory flow batteries.

The key quantity for predicting charge transfer rate is therefore the solvation (intermolecular) λ contribution. First we consider a single Fl molecule solvated in CH_3CN. The standard CFMD approach to compute λ, derived from rigorous statistical mechanics, is to generate a trajectory using each of the Fl and Fl^- Hamiltonian. The distributions of gap

FIG. 6: (a) Fitted parabolic curves for Fl→Fl$^-$ reorganization energy as the solvation coordinate varies. (b) Same as (a), but for Fl and Fl$^-$ adsorbed on graphite electrode surface. The Fl$^-$ is frozen in a flat geometry.

energies,

$$P_{q'}(x) = \langle \delta[x - \Delta E_{\rm gap}(q=-1) - \Delta E_{\rm gap}(q=0)] \rangle_{q'} \, . \tag{5}$$

are sampled using these trajectories. Here $q' = 0$ or $q' = -1$, and the averages ("$\langle \cdot \rangle_{q'}$") denote sampling over CFMD trajectories with the target molecule in the two different q' state. The two $\log P_{q'}(x)$ predicted are expanded about their minima, fitted to parabolas, and multipled by the thermal energy $k_{\rm B}T$. The bottom of these parabolas are aligned to mimic equilibrium (no driving force or overpotential, i.e., $\eta = 0$) conditions. Their intersection yields $4 \times \lambda$.

In the bulk CH_3CN solution with a single Fl molecule, λ=1.76 eV. See Fig. 6a. This is a fairly standard value for the solvent contribution to λ. If the pre-exponential factor in Eq. 4 is 10^6/s, this λ yields a 150/s electron transfer rate.

Our interfacial simulation cell allows us to consider the heterogeneous e^- transfer rate for Fl molecules near the electrode surface. Both V_o and λ depend on the location and orientation of the Fl molecule. Here we focus on Fl directly adsorbed on graphite at a $\sim$-0.9 V EDL configuration, when Fl should be electrochemically reduced. As discussed above, charge-neutral Fl preferentially adsorbs on the surface but Fl$^-$ is tilted on the surface (Fig. 4c). To conduct a consistent calculation, we freeze Fl$^-$ flat on the electrode surface. The resulting λ in this configuration is 0.64 eV (Fig. 6b). This is much lower than the 1.76 eV computed in the bulk region of CH_3CN liquid. The reason is the proximity of the metallic electrode, which exhibits a large high-frequency dielectric constant ϵ_∞. In modeling terms, the instantaneous change in Fl charge state is "solvated" by its image charge on the electrode. This accommodates the electron transfer and drastically reduces the e^- transfer barrier. In contrast, solvent molecules cannot solvate the sudden change in electron density because of the finite solvent molecule orientation and ion diffusion times. This point has been made in the literature.[15,16] Without our image-charge implementation, we would not have observed this phenomenon. If the pre-exponential factor in Eq. 4 is 10^6/s, $\lambda = 0.64$ eV yields a 7×10^3/s electron transfer rate, much faster than that inside bulk liquid CH_3CN.

The e^- transfer rates discussed in this section are ensemble-averaged. A more direct demonstration of Fl electrochemical reduction is to consider its energetics in real time. To

remove an electron from graphite and put it on Fl, the *electronic* energy cost (not included in CFMD simulations) is the difference between the graphite work function and the Fl gas phase electron affinity: $(4.40 - 1.17) = 3.23$ eV. The solvation energy difference ("energy gap," Eq. 5) between the Fl and Fl^- states is needed to overcame this energy to permit electron transfer. This solvent contribution, sampled on the uncharged Fl electronic ground state charge Hamiltonian, implicitly includes the $-0.9\ V$ via the electrode image charges and the electric double layer.

Fig. 7 depicts this energy gap as a function of time along the CFMD trajectory. The instances where this function crosses the red line (-3.23 eV) indicate when Fl $\rightarrow$ Fl^- is favorable. This occurs about 10 times in the 50 ps trajectory, which indicates that it is possible to perform CFMD simulations that switch the identity of Fl and Fl^- in real-time CFMD simulations. In the original proposal, we advocate using the Monte Carlo algorithm approach, so that exact conservation of energy is not necessary for such switching. In practice, hybrid MD/MC runs will need a means to impose a constant voltage *from time step to time step* (see the Method section). Otherwise, the net change of a neutral molecule to an anion will induce an extra $+|e|$ image charge in the electrode. In this finite sized simulation cell, modifying the electrode surface charge in this way would induce a voltage change of at least +0.2 V, thus drastically varying the electrochemical condition of the simulation cell as Fl reduction proceeds. Hence MC methods will be deferred to future studies after further code and method development.

4. DISCUSSIONS

In this section, we discuss future technical work and deviations from our original proposals.

Estimation of the absolute electron transfer rate requires V_o, which is a function of the distance between the electrode and the molecule accepting e^-, as well as the molecular orientation. Large V_o results in adiabatic electron transfer, which is the condition considered in metal plating simulations by Schmickler et al.[17] Small V_o is consistent with non-adiabatic e^- transfer (Eq. 4). Along the trajectory discussed in Fig. 7, at the crossing point of the red and red lines, i.e., when e^- transfer energy is conserved, the probability of transition between Fl and Fl^- is subject to the Landau-Zener formula, which also depends on the magnitude of V_o.

We have attempted to estimate V_o between graphite and Fl using the approach of

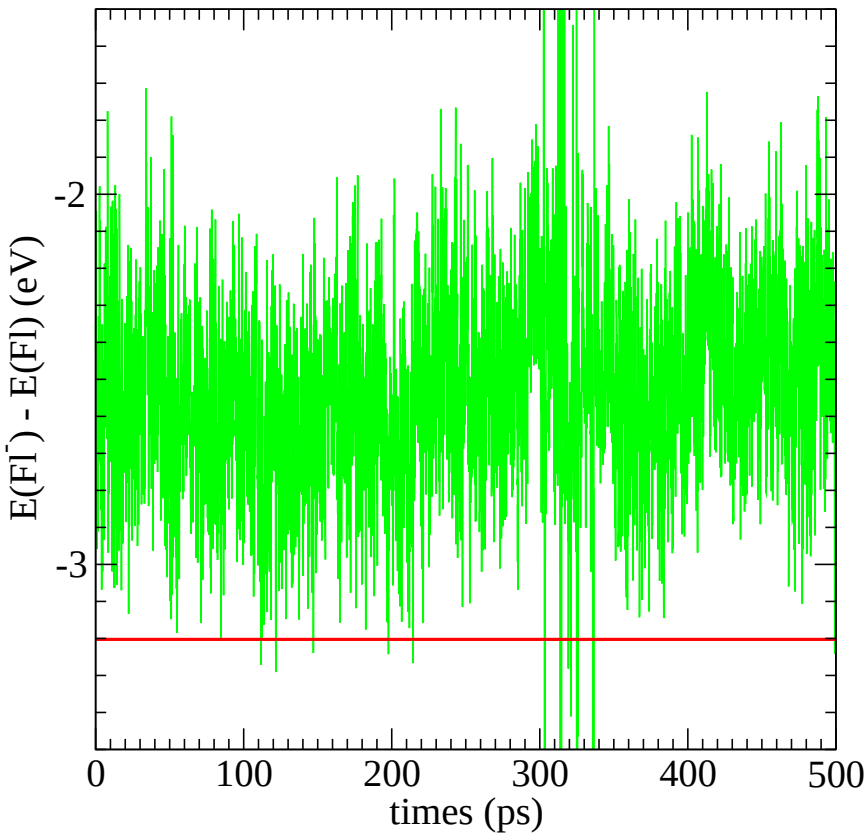

FIG. 7: Fl "gap" energy, $\langle E(q=-1) - E(q=0) \rangle_{q=0}$ as a function of time. Below red line, electron transfer to Fl and to form Fl^- is energetically favorable.

Schmicker *et al.*[17] The value proves too small ($< 0.001\ eV$) to be effectively estimated using this method. A quantum chemistry cluster method will be applied in the future, although it is a concern that such an approach may yield a large, unphysical graphite band when graphite is metallic in reality. For the purpose of conducting CFMD simulations that switch the identities of Fl and Fl^-, knowledge of V_o is not absolutely necessary. One can assume maximal electron transfer, i.e., Fl will transform into Fl^- any time it is energetically favorable to do so (Fig. 7). Note that e^- cannot occur even for large V_o if the energy matching criterion is not met within a few units of thermal energy ($k_B T$.) Thus the more urgent task is to implement a way to keep the anode potential the same from time step to time step.

During our one-year project, new discoveries has led to modification of several technical approaches. For example, use of the Siepmann-Sprik constant voltage method, implemented

into LAMMPS by external researchers, proves problematic. It does not lead to charge neutrality in the simulation cell. Furthermore, initialiation of the method for a 6000-atom system takes about 5 minutes on 64 processors because of the need to minimize the variable charges on each electrode atom. In subsequent time steps, the cost is much lower, but the initialization cost makes it prohibitive for some of our applications. Therefore we have switched to image-charge constant-potential method described at length above.

As discussed in Sec. 3, initial AIMD simulations of ferrocenium (Fc^+) and its derivative in the electrolyte give erroneous results. This issue has been subsequently resolved by imposing a low-spin Fe(III) electronic configuration, and some MD simulations of Fc' are reported herein. For this reason, for the purpose of benchmarking the modified LAMMPS code, fluornone (Fl) is used as a proof-of-principle redox-active species, and most of the simulations pertain to Fl. This planar molecular has never been modelled in an electrochemical context, and the predictions associated with it prove interesting and novel.

5. ANTICIPATED IMPACT

Atomic lengthscale modeling of flow battery components are arguable in its infancy. The published work mostly consist of electronic calculations on anolyte/catholyte solvation[5] or classical force field molecular dynamics of the liquid electrolyte by itself to investigate its viscosity.

Our simulations focus on the hitherto neglected area of electrode/electrolyte interfaces. Our results on how the fluorenone adsorption geometry changes a function of applied voltages. They are of sufficiently novelty to be published, perhaps after investigating system size effects. This work will also be presented in a Nanostructure for Electrical Energy Storage (NEES) Energy Frontier Research Center (EFRC) teleseminar in December. One goal of this seminar is to introduce a subset of the EFRC principal investigators, who are experts in nanofluidics, to redox flow battery research. RFB research can benefit from their expertise. Other presentations of this work will be considered at Materials Research Society or American Chemical Society conferences to raise the profile of atomic lengthscale modeling of flow batteries.

In a broader context, our work establishes a protocol for modeling liquid/solid interfaces relevant to flow batteries. Flow batteries differ from, say, electrochemical capacitors, in that the voltage imposed on electrodes must be correlated with the redox states of the catholytes and anolytes. The voltage do not only affect mass transport in the liquid, but also the

concentrations of the redox active species at different charge states. Our approach to deal with the added complexity is to use minimal amount of electronic calculation to compute the electrode work function and anolyte electron affinity. DFT calculations give the energy cost of electron transfer in vacuum for a charge-neutral electrode. The effect of adding the liquid electrolyte and a net charge on the electrode surface are included sequentially using classical force field simulations (Fig. 1). A centerpiece of the methodology is the implementation of the image charge technique into the Sandia LAMMPS alongside Ewald summation to deal with long-range electrostatics.

Image-charge techniques are also applicable to solid state electrolytes and their interfaces with solid electrodes. We are currently working on implementing this method into a coarse-grained Ising model designed for solid-solid interface applications, to be parameterized using DFT predictions. The use of such models are necessary to incorporate finite temperature effects and variable Li-content as a function of voltage at all-solid-state battery interfaces.

In terms of programmatic impact on redox flow battery research, understanding the interfacial structure (the electric double layer) as a function of voltage yields insights about charging rates and degradation behavior. For example, our discovery that the active site (oxygen) of Fl^- tilts away from the electrode strongly suggests that degradation does not occur vi Fl^- reaction with the electrolyte. The ensemble-averaged electron transfer rate can be computed after considering multiple redox species adsorption configurations and estimating the relevant electron tunneling matrix elements (V_o in Eq. 4). The elucidation of the absolute charge transfer rate will aid design of new redox-active species for flow batteries and assist the economics analysis of whether such batteries are viable.[3]

We will discuss our modeling results and capability with researchers and funding agencies that coordinate research on organic solvent-based redox flow batteries, including Organization 2500 in Sandia, the Department of Energy Office of Electricity (DOE/OE), Pacific Northwest Laboratory (which is the DOE/OE project lead on RFB), and JCESR.

6. CONCLUSIONS

In conclusion, we have used atomic lengtshcale modeling techniques to study organic-solvent-basesd anolytes and catholytes at graphite interfaces in this exploratory LDRD. The bulk of the simulations involve fluorenone (Fl) as anolyte, and reveal significant changes in Fl adsorption geometry as the anode potential decreases towards the Fl reduction voltage. The reorganization energy is lower for Fl adsorbed on the electrode than Fl solvated in the

bulk electrolyte by more than 1 eV, suggesting that electron transfer should be faster by a factor of 5×10^4 even if the tunneling matrix element V_o is unchanged.

Our simulations apply classical force field-based molecular dynamics (MD) augmented by a small amount of DFT calculations. They establish a protocal for modeling redox flow battery interfaces during steady-state charge and discharge conditions, when the anolyte or catholyte, present at high concentration, can undergo redox reactions. In particular, we have implemented a version of the image-charge technique for a single electrode into Sandia's LAMMPS MD code which permits modeling the electrode as having a constant potential on its surface. Further improvement and application of this technique is expected to have impact on multiple electrochemistry-related Sandia programs.

[1] Skyllas-Kazacs, M.; Chakrabarti, M.H.; Hajimolana, S.A.; Mjalli, F.S.; M. Saleem. *J. Electrochem. Soc.* **2011**, *158*, R55-79.

[2] Parasuraman, A.; Lim, T.M.; Menictas, C.; Skyllas-Kazacos, M. *Electrochim. Acta* **2013**, *101*, 27-40.

[3] Darling, R.M.; Gallagher, K.G.; Kowalski, J.A.; Ha, S.; Brushett, F.R. *Energy Environ. Sci.* **2014**, *7*, 3459.

[4] Li, B.; Gu, M.; Xie, Z.; Wei, X.; Wang, C.; Sprenkle, V.; Wang, W. *Nano Lett.* **2014**, *14*, 158-165.

[5] Sepehr, F.; Paddison, S.J. *Chem. Phys.* **2013**, *585*, 53-58.

[6] Han, K.S.; Rajput, N.N.; Wei, X.; Wang, W.; Hu, J.Z.; Persson, K.A.; Mueller, K.T. *J. Chem. Phys.* **2014**, *141*, 104509.

[7] Cosimbescu, L.; Wei, X.; Vijayakumar, M.; Xu, W.; Helm, M.L.; Burton, S.D.; Sorensen, C.M.; Liu, J.; Sprenkle, V.; Wang, W. *Scientific Reports* **2014**, *5*, 14117.

[8] Wei, X.; Xu, W.; Huang, Zhang, L.; Walter, E.; Lawrence, C.; Vijayakumar, M.; Henderson, W.A.; Liu, T.; Cosimbescu, L.; Li, B.; Sprenkle, V.; Wang, W. *Angew. Int. Ed.* **2015**, *54*, 8684-8687.

[9] Frisch, M.J.; *et al.*, Gaussian 03 (Revision C.02), Gaussian Inc., Wallingford, CT, 2004. See the electronic supporting data (ESD) for more details.

[10] Kresse, G.; Furthmüller, J. *Phys. Rev. B*, **1996**, *54*, 11169; *Comput. Mater. Sci.*, **1996**, *6*, 15.

[11] Kresse, G.; Joubert, D.; *Phys. Rev. B*, **1999**, *59*, 1758.

[12] Perdew, J.P.; Burke, K.; Ernzerhof, M. *Phys. Rev. Lett.*, **1996**, *77*, 3865.

[13] Torrie, G.M.; Valleau, J.P.; Patey, G.N. *J. Chem. Phys.* **1982**, *76*, 4615.

[14] Böhn, H.J.; McDonald, I.R.; Madden, P.A. *Mol. Phys.* **1983**, *49*, 347-360.

[15] Reed, S.K.; Madden, P.A.; Papadopoulos, A. *J. Chem. Phys.* **2008**, *128*, 124701.

[16] Nikitina, V.A.; Kislenko, S.A.; Nazmutdinov, R.R.; Bronshtein, M.D.; Tsirlinna, G.A. *J. Phys. Chem. C* **2014**, *118*, 6151-6164.

[17] Pinto, L.M.C.; Quaio, P.; Santos, E.; Schmickler, W. *ChemPhysChem*, **2014**, *15*, 132-136.